1. Experimental Section

Chemicals and reagents.

Cobalt nitrate hexahydrate (98%, Aladdin), 2-methylimidazole (99%, J&K), methanol and ammonium molybdate (analytical grade, Tianjin Chemical Reagent Wholesale Company), KOH (analytical grade, Aladdin). Ultrapure water (Millipore, 18.25 MΩ cm) was used throughout all experiments. All chemicals were directly used without any purification.

Material synthesis

1.3 g 2-methylimidazole was dissolved in 40 ml deionized water and stirred for 2 h (Solution A). 0.58 g cobalt nitrate hexahydrate and 0.26 g ammonium molybdate were dissolved in 40 ml deionized water and continually stirred for 2 h (Solution B). Then, solution A was quickly poured into the solution B with further stirring for 5 min. A piece of acid-treated carbon cloth (CC) was added into the mixture solution. After reaction for 4 h, the sample was taken out, washed with deionized water and dried at 60^{o}C under vacuum for 12 h (Co-ZIF-MoO_4/CC).

A piece of Co-ZIF-MoO_4/CC was firstly heated at 250°C with a ramp rate of 1°C min^{-1} and kept at 250°C for 2 h under air atmosphere. Afterward, the calcined sample was putted into a tube furnace system and nitridation at 370^{o}C, 420^{o}C and 470^{o}C for 2 h with a heating rate of 5^{o}C min^{-1} under an NH_3 atmosphere (30 sccm), the achieved samples were assigned to be Mo-Co_4N-N_{370}, Mo-Co_4N and Mo-Co_4N-N_{470}. Co_4N, Mo_{low}-Co_4N and Mo_{high}-Co_4N were prepared via the same procedure of Mo-Co_4N expect 0 g, 0.13 g and 0.39 g ammonium molybdate were added, respectively. The loading amount of Co_4N and Mo-Co_4N on carbon cloth were about 1.5 mg cm^{-2}. A

mixture of Pt/C (20 wt%, 2 mg), 40 μl Nafion solution (5 wt%) and 960 μl isopropanol was sonication for 2 h to form a homogenous dispersion, which was then loaded into a piece of carbon cloth with the loading of Pt/C catalyst was 0.5 mg cm^{-2}.

Materials Characterization.

X-ray diffraction (XRD) was conducted by using Cu Ka radiation (Rigaku D/Max-2500). Scanning electron microscopy (SEM) and transmission electron microscopy (TEM) were performed with JEOL JSM-7500F and Talos F200X G2 AEMC instruments, respectively. X-ray photoelectron spectroscopy (XPS) was carried out by using a ThermoFischer ESCALAB 250Xi. The formate was detected by ion chromatography (IC, ThermoFischer Aquion). Inductive coupled plasma mass spectrometry (ICP-MS) was conducted to study the elemental composition using a SPECTRO-BLUE. X-ray absorption near-edge structure (XANES) tests were collected at the photoemission end-station at beamline BL10B in the National Synchrotron Radiation Laboratory (NSRL) in Hefei, China. All the XANES spectra were calibrated based on the Au 4f of a freshly sputtered gold wafer. All static calculations were carried out using DFT with generalized gradient approximation of Perdew-Burke-Ernzerhof as implemented in VASP 5.4.4 code.

Electrochemical Measurement.

The electrochemical measurements were performed by a CHI 760E electrochemical station (Shanghai Chenhua, China). The as-prepared samples, graphite rod and saturated calomel electrode (SCE) were used as work electrode, counter electrode and reference electrode, respectively. Linear sweep voltammetry (LSV) was

tested 5 mV s^{-1} for the polarization curves. For double-layer capacitances (C_{dl}) measurements, different scanning rates of 5, 10, 15, 20, 25, 30, and 40 mV s^{-1} of CV cycling in the range of non-faradic district were performed. The ECSA is acquired from the C_{dl} based on the equation:

$$ECSA = C_{dl}/C_s$$

where C_s is the specific capacitance of the catalyst. From the literature, the value of C_s was 0.040 mF cm^{-2} in this work. The electrochemical impedance spectroscopy (EIS) measurements were collected with frequencies ranging from 100 KHz to 0.1 Hz. The above-mentioned electrochemical data was presented with 95% iR compensation. TOF values were measured and based on the following equation: TOF = j/(2Fn), in which j is the HER current density, n is the number of active sites, and F is Faraday constant. The n values were measured and computed by cyclic voltammetry (CV) recorded between 0-0.6 V vs RHE in 1 M KOH at a scan rate of 50 mV s^{-1}. Then, by integrating the charge of each CV curve over the whole potential range, the half value of the charge was obtained as the surface charge density (Q). The n value could be calculated by the follow equation: n = Q/F.

For the two-electrode HER/MOR electrolyzer, the as-prepared samples were used as both the anode and cathode. The Faraday efficiency (FE) of H_2 and formate can be calculated by the following equations:

$$FE(H_2) = \frac{n \times 2 \times N_A \times e}{Q} \times 100\%$$

$$FE(\text{formate}) = \frac{n \times 4 \times N_A \times e}{Q} \times 100\%$$

where n is the mol of generated H_2 or formate, N_A is Avogadro constant (6.02×10^{23} mol^{-1}), e is elementary charge (1.60×10^{-19} C), Q is the amount of electricity passed (C).

2. Supplementary Figures and Tables

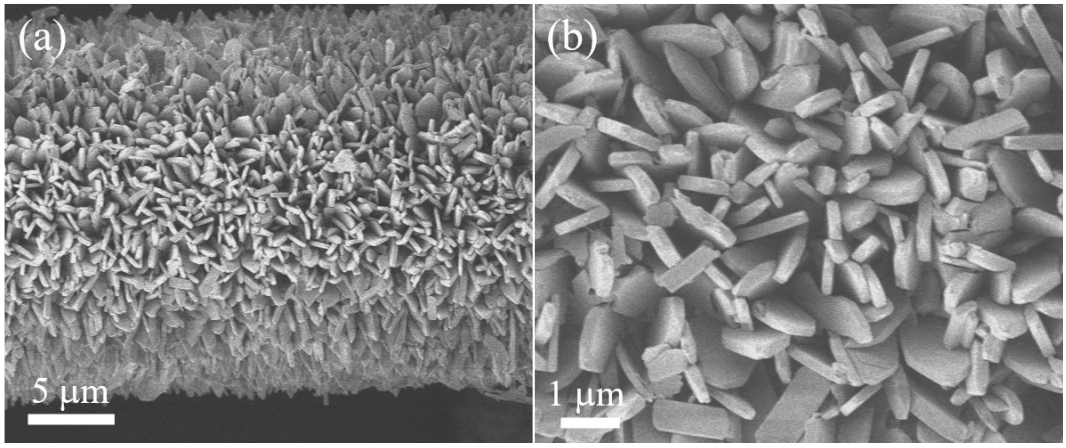

Figure S1. SEM images of Co-ZIF/CC.

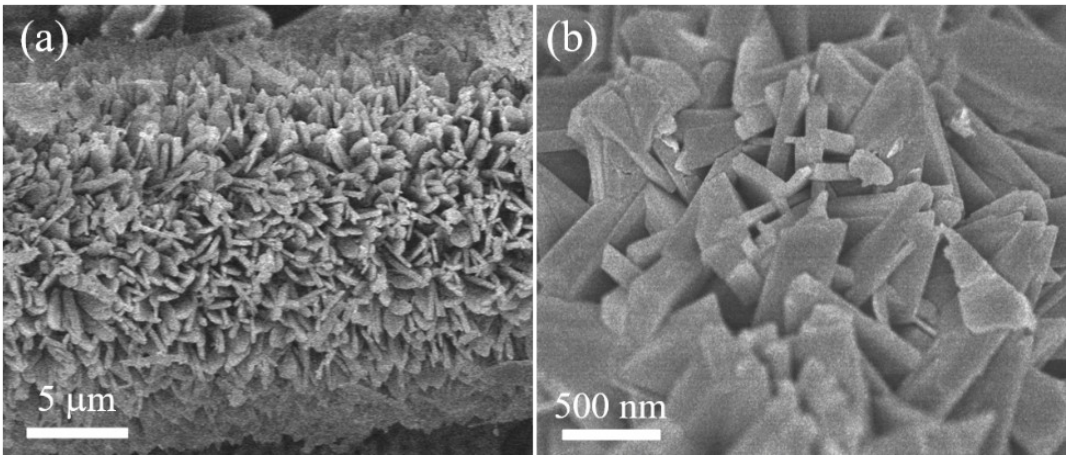

Figure S2. SEM images of Co-ZIF-MoO_4/CC.

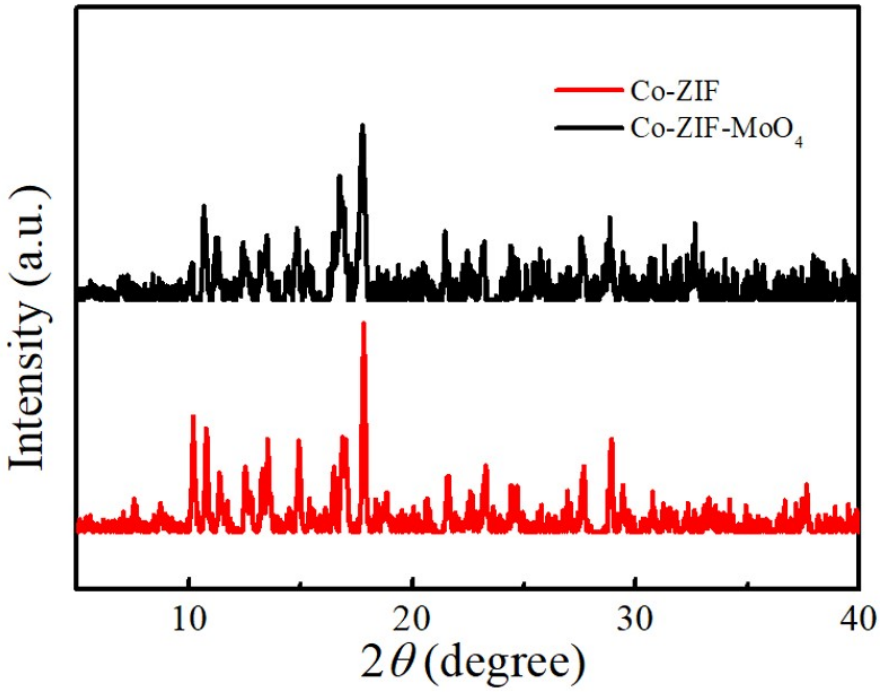

Figure S3. XRD patterns of Co-ZIF and Co-ZIF-MoO_4.

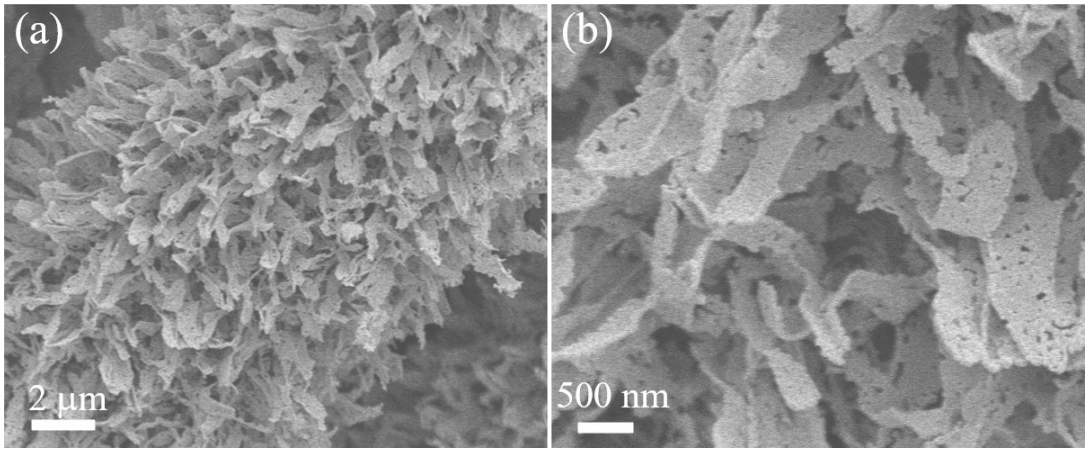

Figure S4. SEM images of Co_4N.

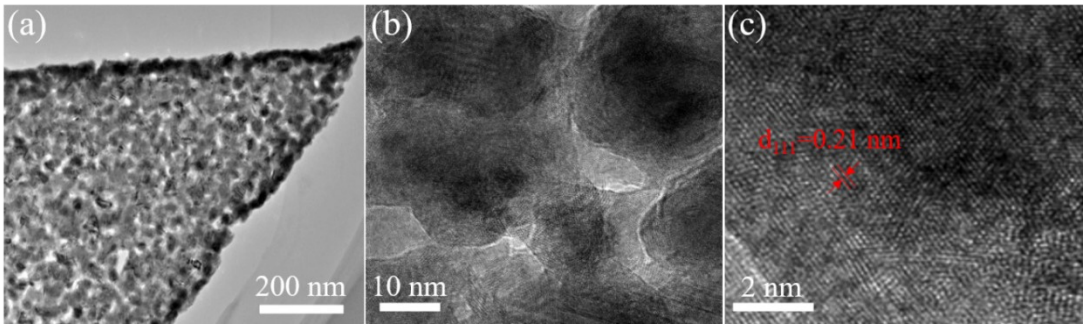

Figure S5. TEM images of Co_4N.

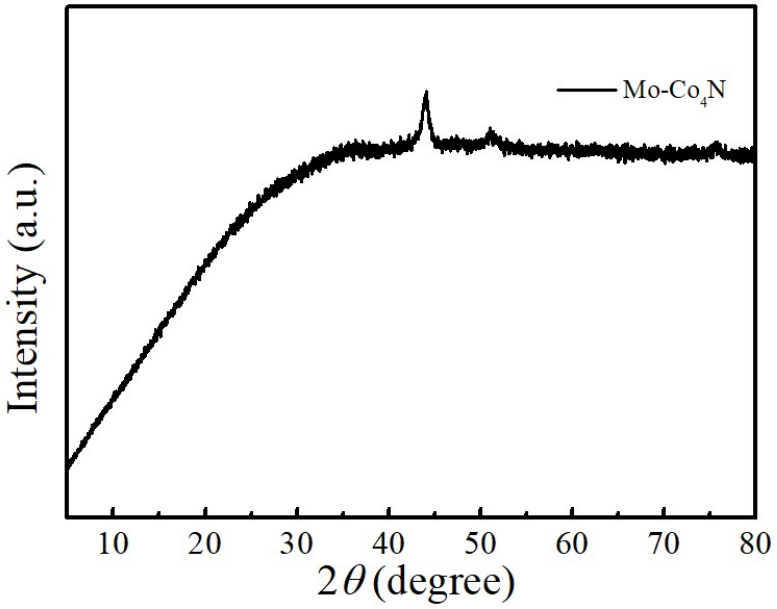

Figure S6. XRD pattern of the as-prepared Mo-Co_4N scraped from carbon cloth substrate.

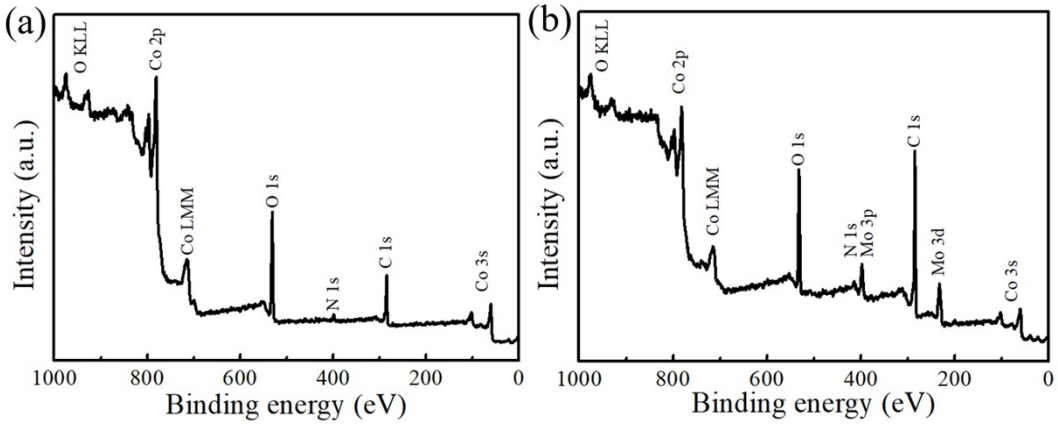

Figure S7. XPS survey spectra of (a) Co_4N and (b) Mo-Co_4N.

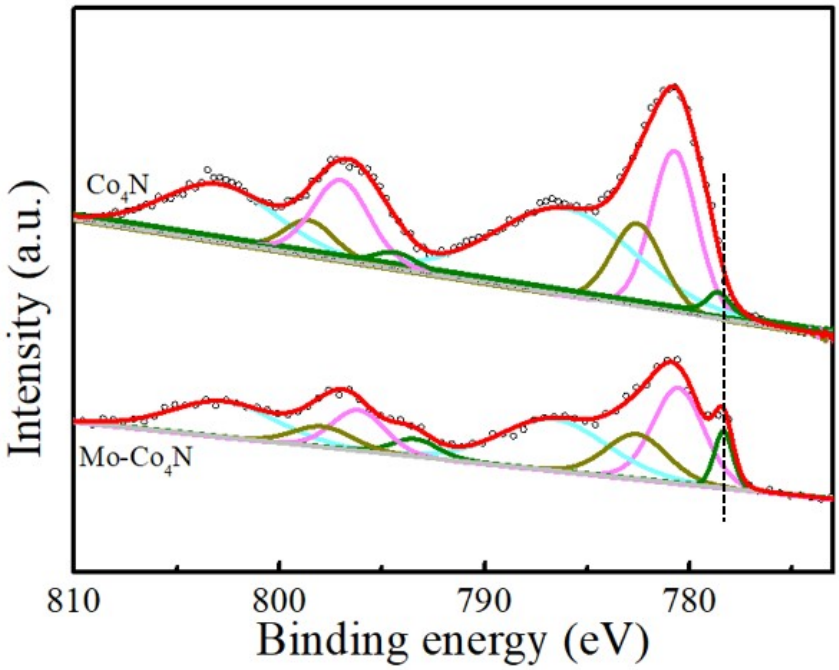

Figure S8. High resolution XPS spectra of Co 2p for Co_4N and Mo-Co_4N.

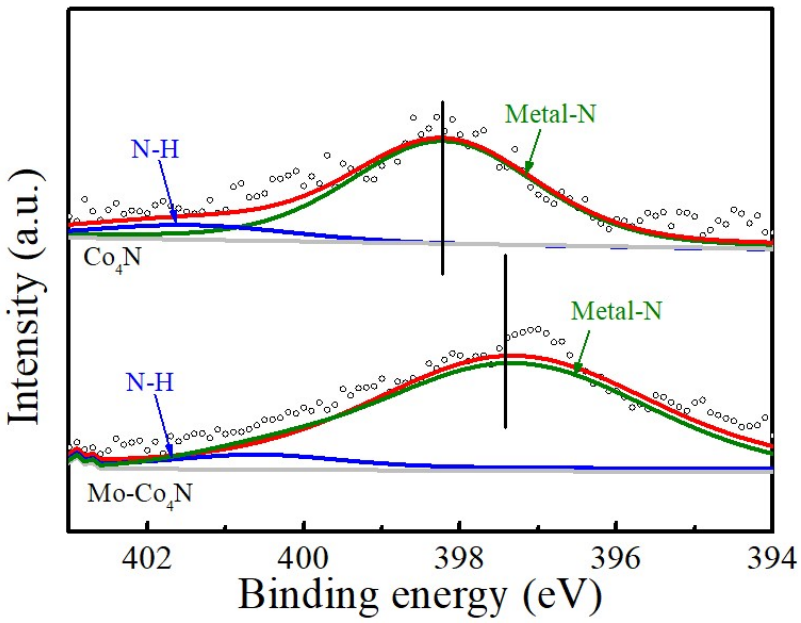

Figure S9. High resolution XPS spectra of N 1s for Co_4N and Mo-Co_4N.

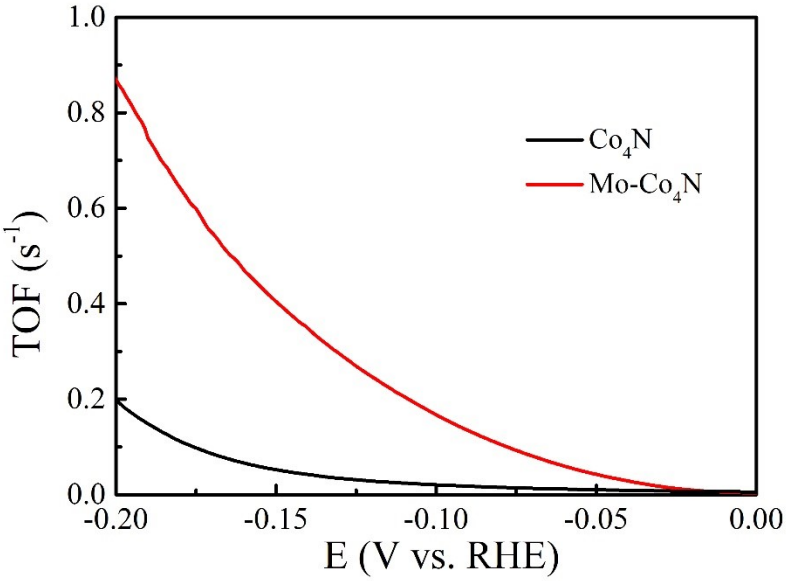

Figure S10. TOF values of Co_4N and Mo-Co_4N for HER.

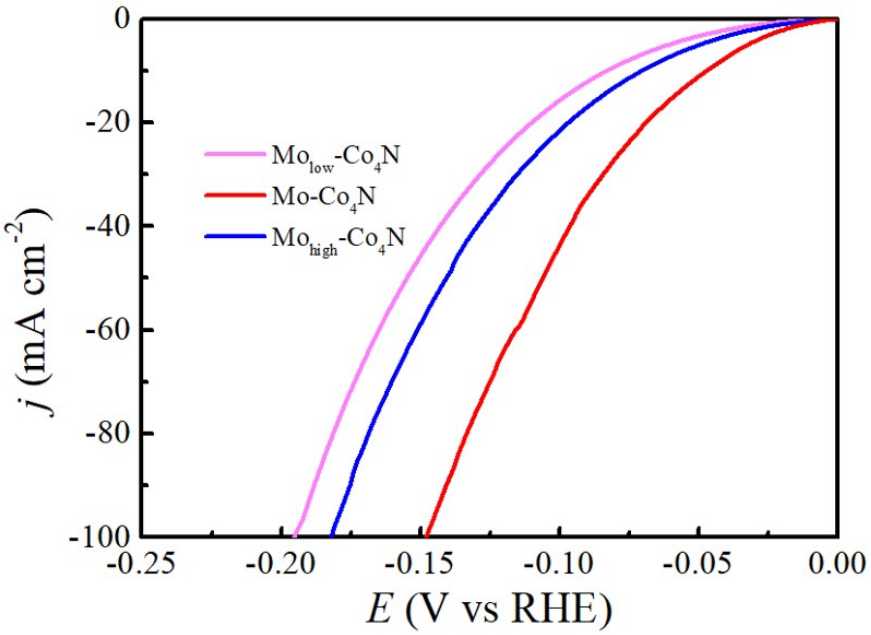

Figure S11. LSV curves of Mo-Co_4N with various dopant ratios for HER.

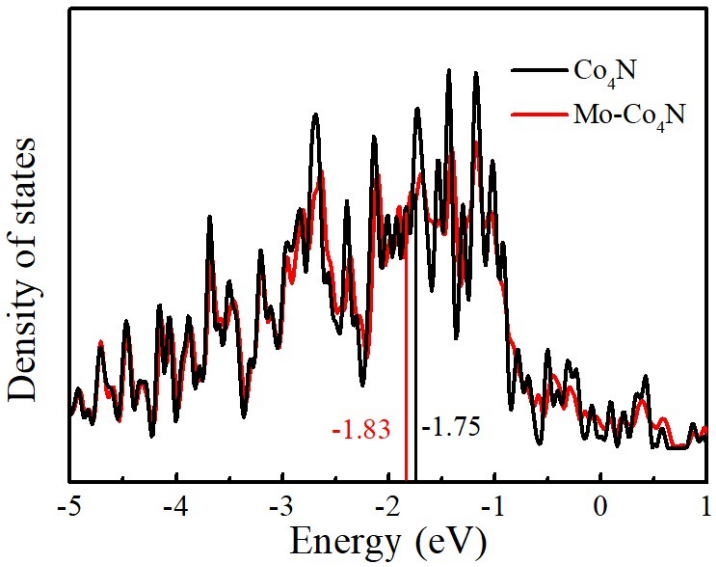

Figure S12. Calculated DOS of Co_4N and Mo-Co_4N and the corresponding d band center potentials.

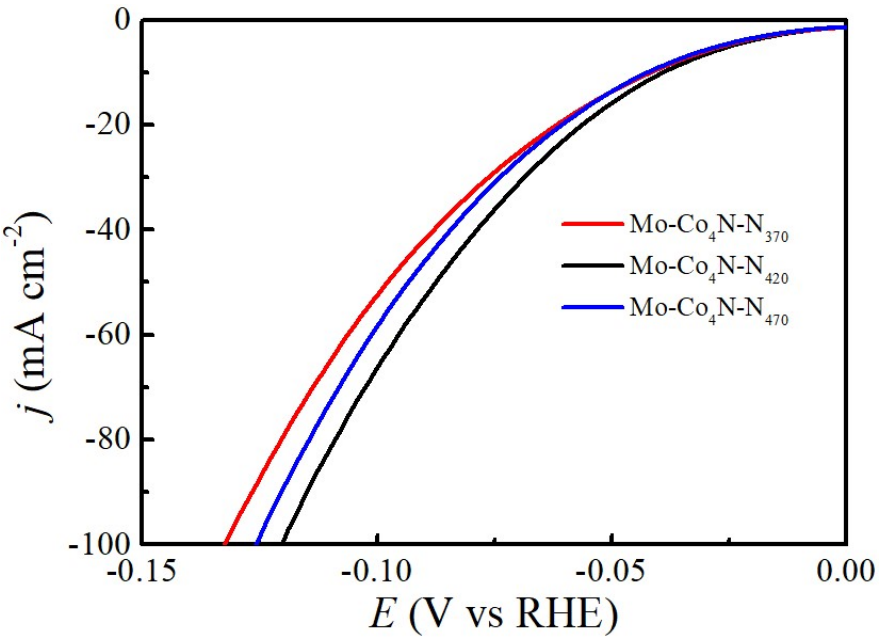

Figure S13. LSV curves of Mo-Co_4N annealed at different temperatures for HER.

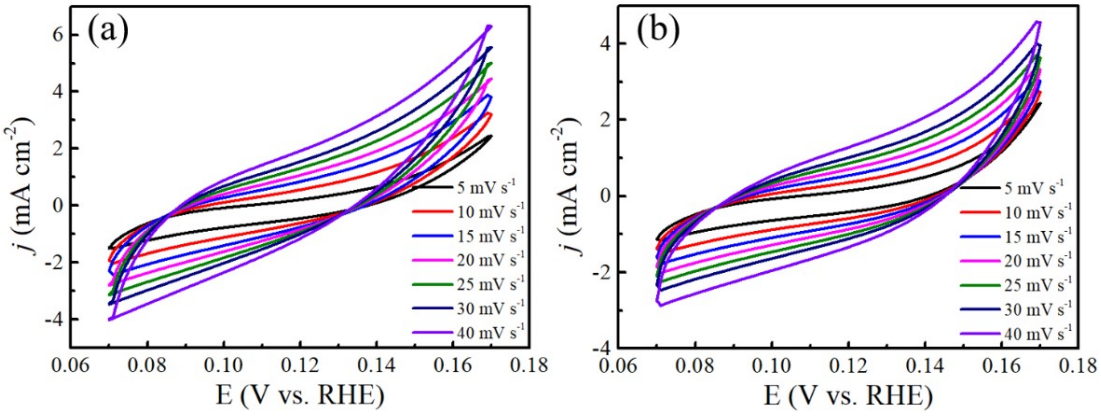

Figure S14. CV curves of a) Mo-Co_4N and b) Co_4N in the double layer capacitive region at the scan rates of from 5 mV to 40 mV s^{-1}.

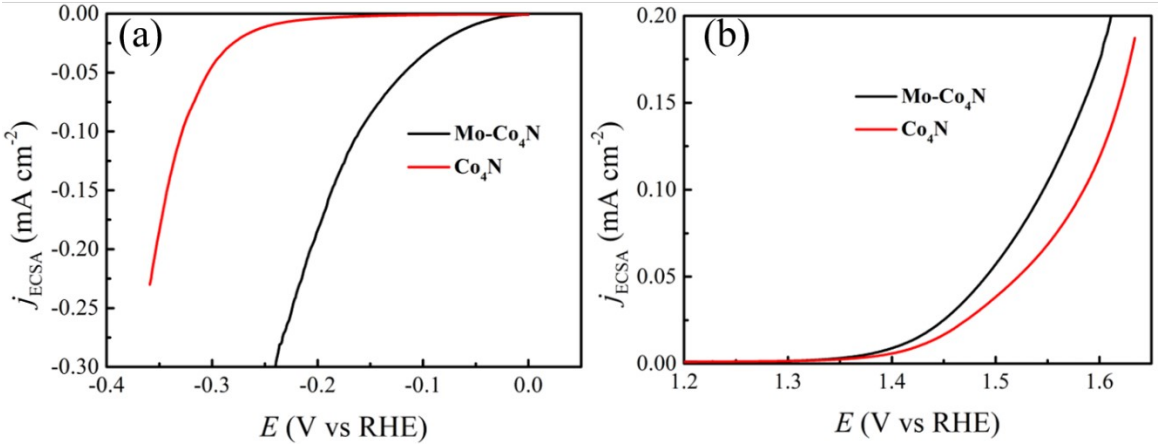

Figure S15. ECSA normalized LSV curves for (a) HER and (b) MOR.

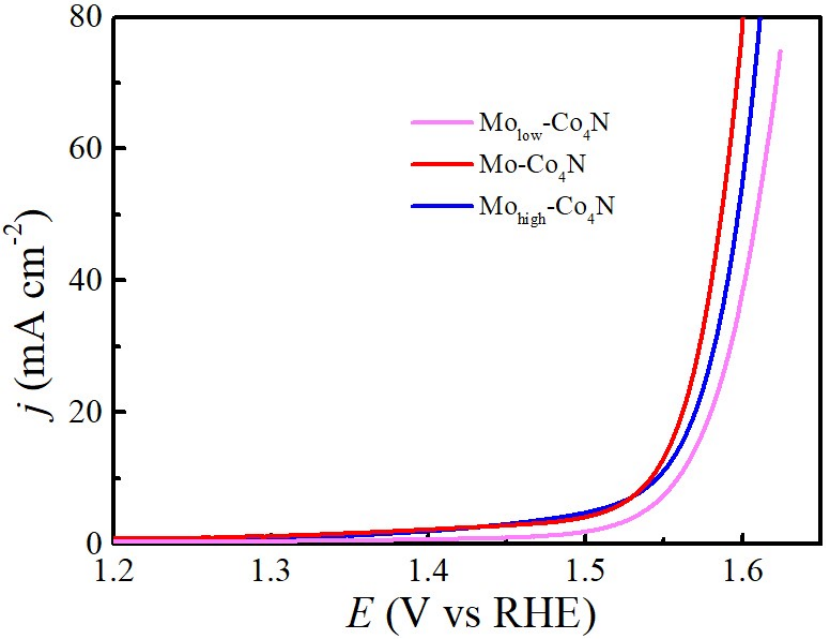

Figure S16. LSV curves of Mo-Co_4N with various dopant ratios for OER.

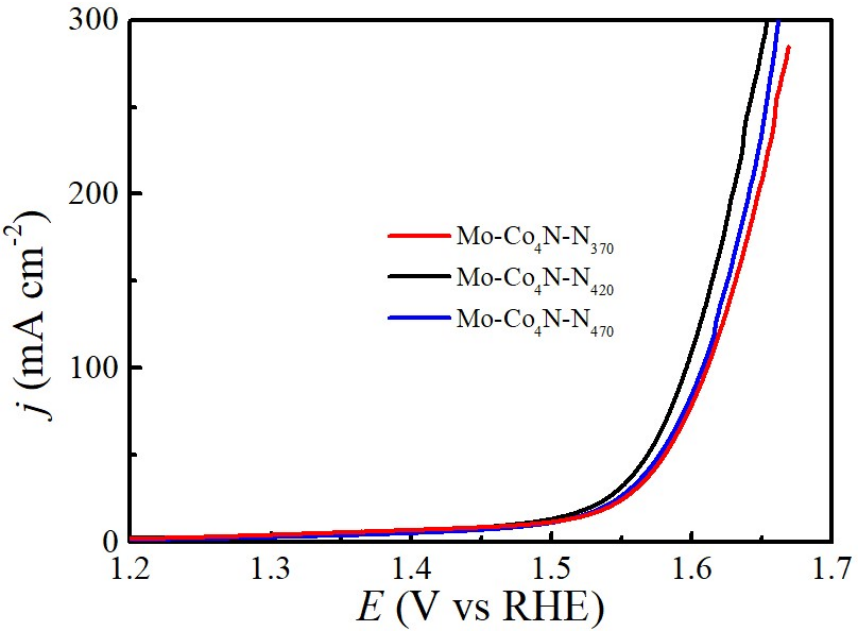

Figure S17. LSV curves of Mo-Co_4N annealed at different temperatures for OER.

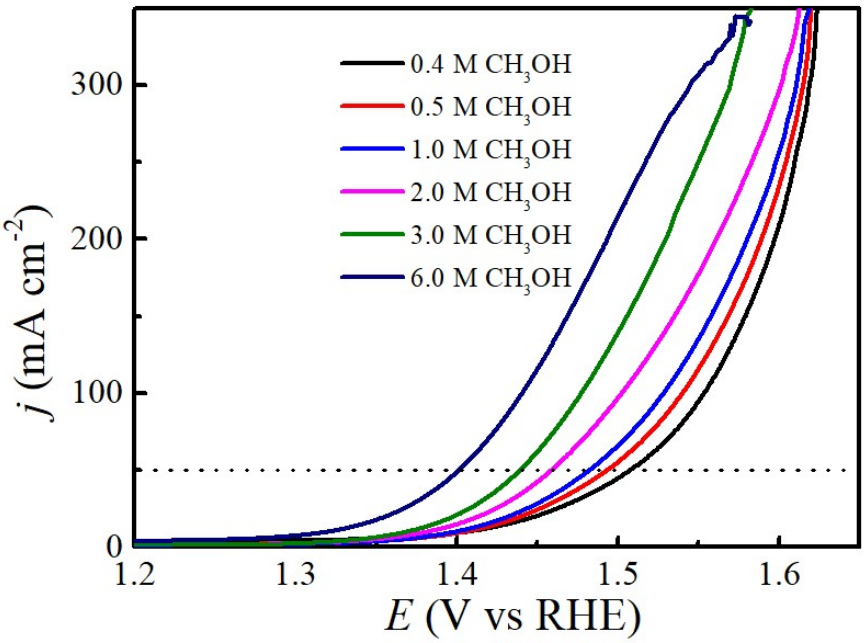

Figure S18. CH_3OH oxidation LSV polarization curves of Mo-Co_4N in 1 M KOH containing different CH_3OH concentrations.

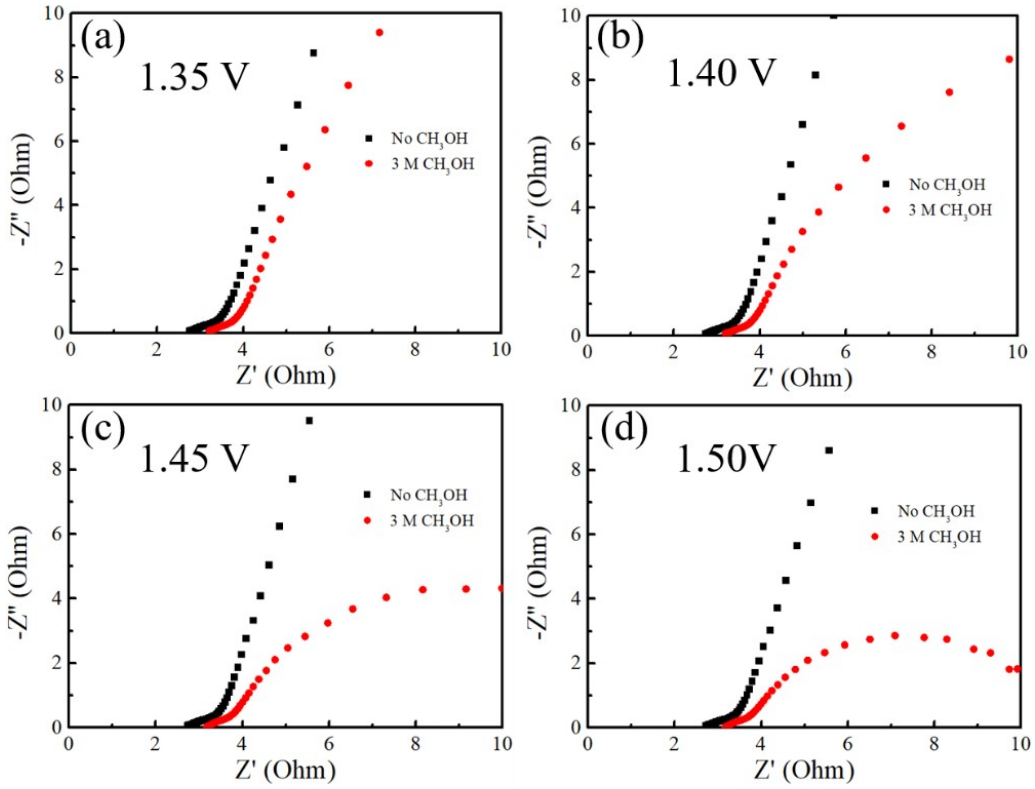

Figure S19. Nyquist plots for Mo-Co_4N in 1 M KOH with and without 3 M CH_3OH at (a) 1.35 V, (b) 1.40 V, (c) 1.45 V, and (d) 1.50 V.

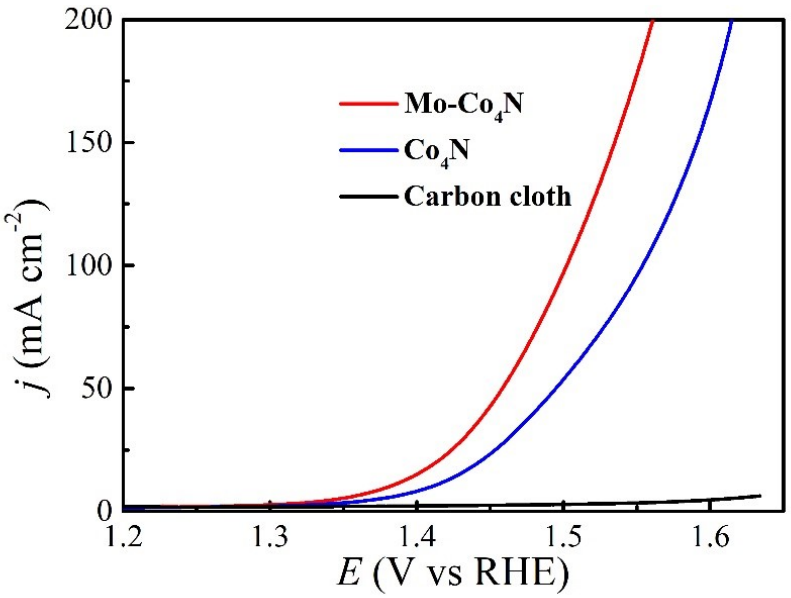

Figure S20. LSV curves of carbon cloth, Co_4N, and Mo-Co_4N for MOR in 1.0 M KOH with CH_3OH.

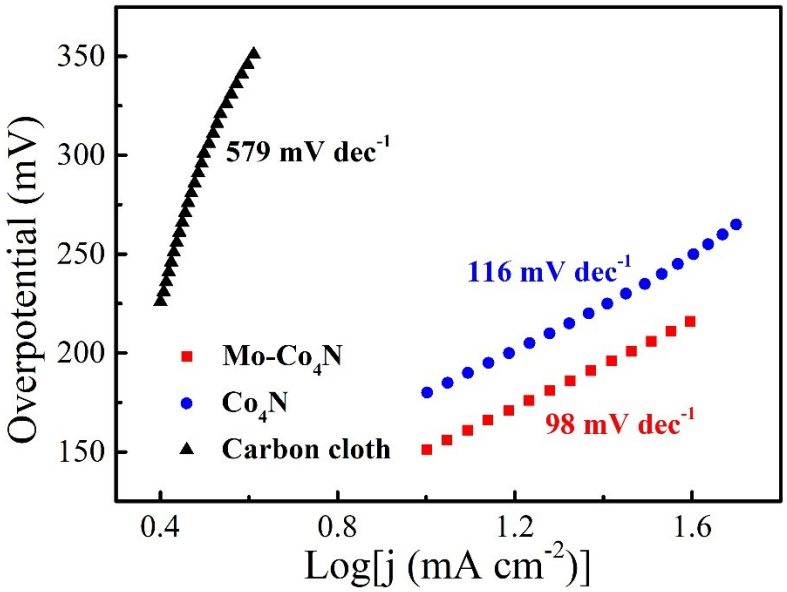

Figure S21. Tafel slope of carbon cloth, Co_4N, and Mo-Co_4N for MOR in 1.0 M KOH with CH_3OH.

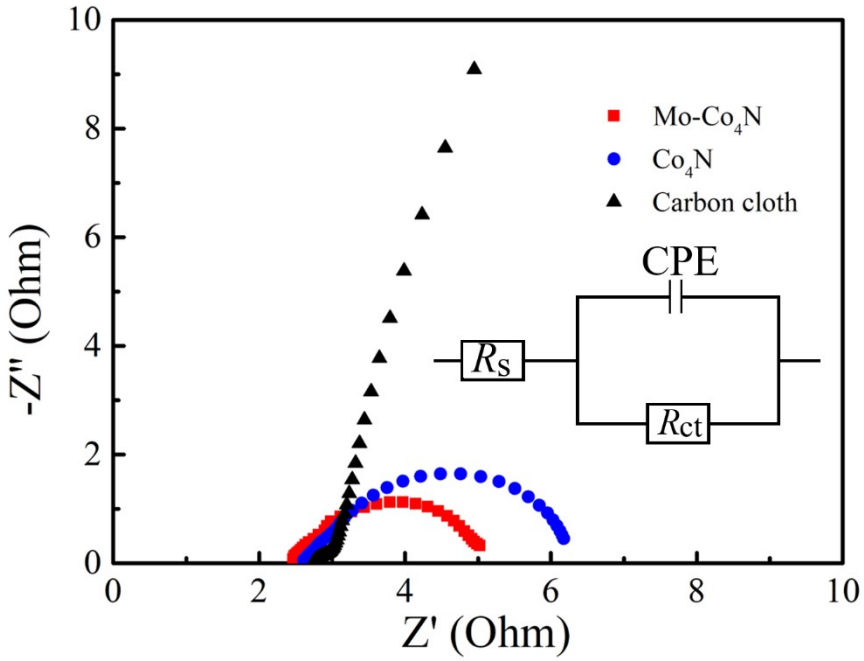

Figure S22. EIS spectra of different samples at potential of 1.5 V. Inset: An equivalent circuit used for fitting data.

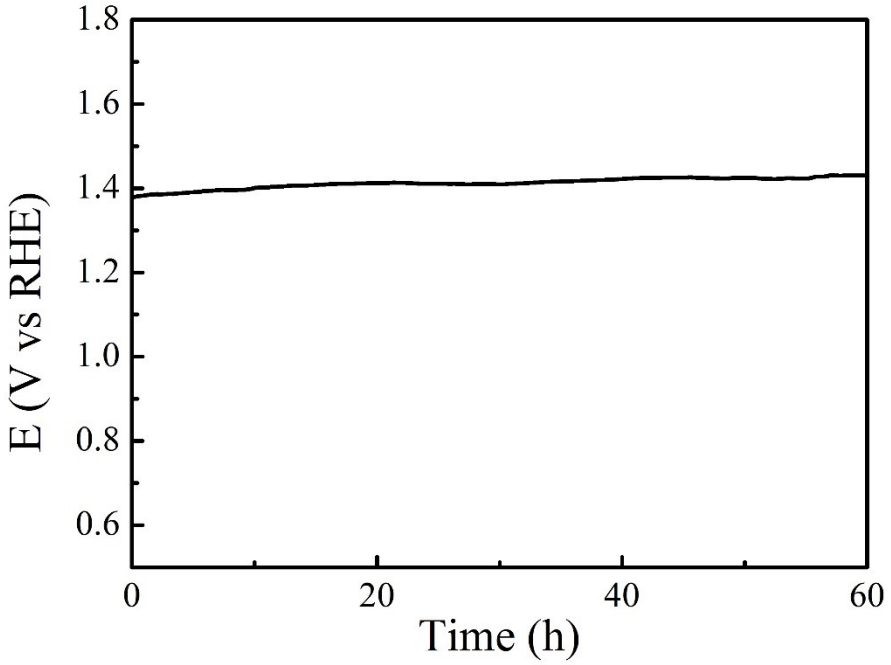

Figure S23. Stability test of Mo-Co_4N at a current density of 10 mA cm^{-2} in 1 M KOH containing 3 M CH_3OH.

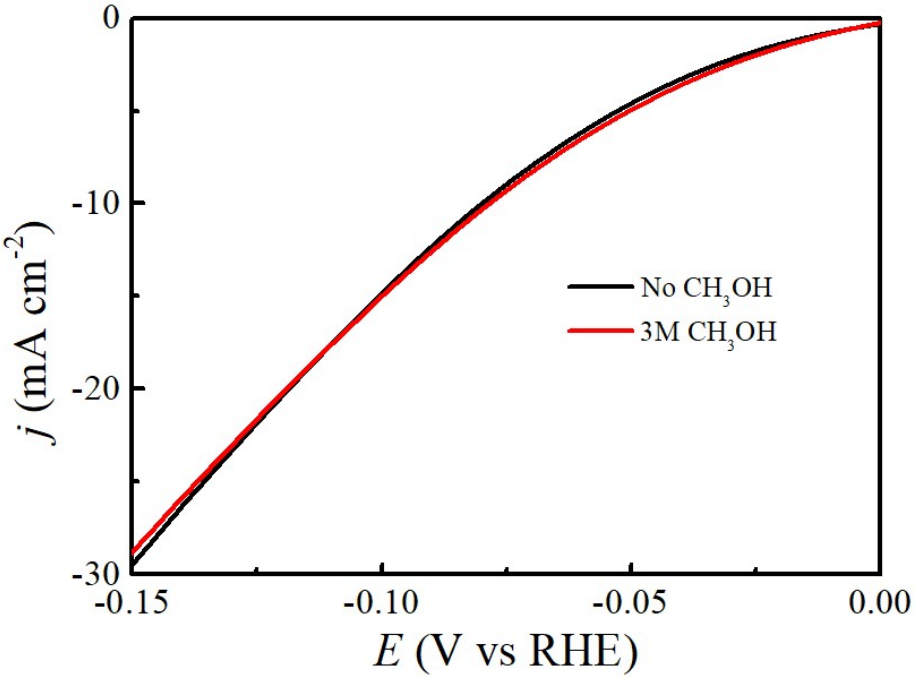

Figure S24. LSV curves of Mo-Co_4N with and without 3 M CH_3OH for HER.

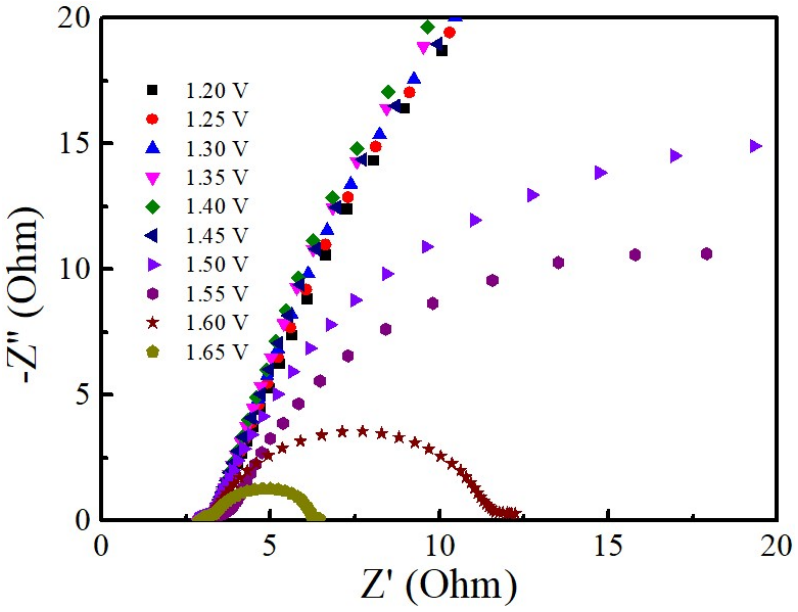

Figure S25. The EIS spectra of Mo-Co_4N at various voltages in 1.0 M KOH.

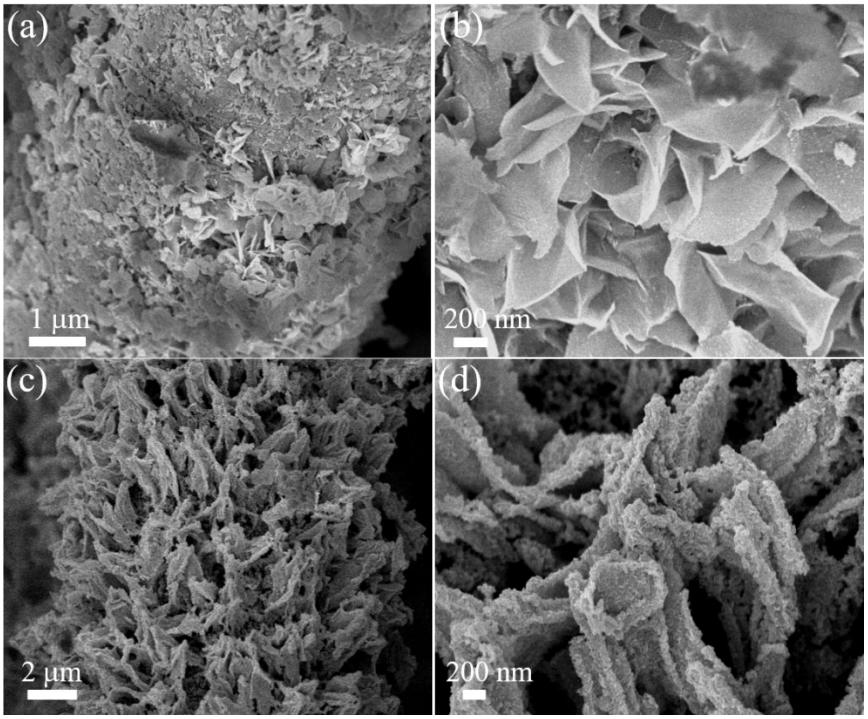

Figure S26. SEM images of Mo-Co_4N after (a,b) HER and (c,d) MOR test.

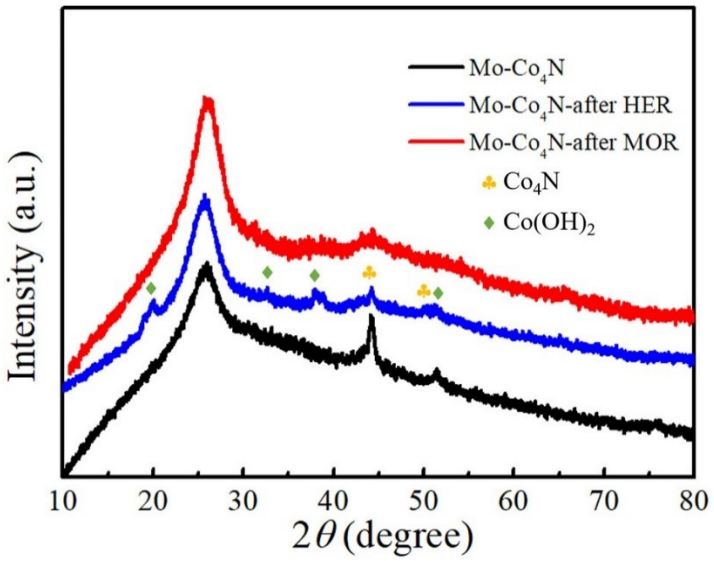

Figure S27. XRD patterns of Mo-Co_4N before and after electrochemical test.

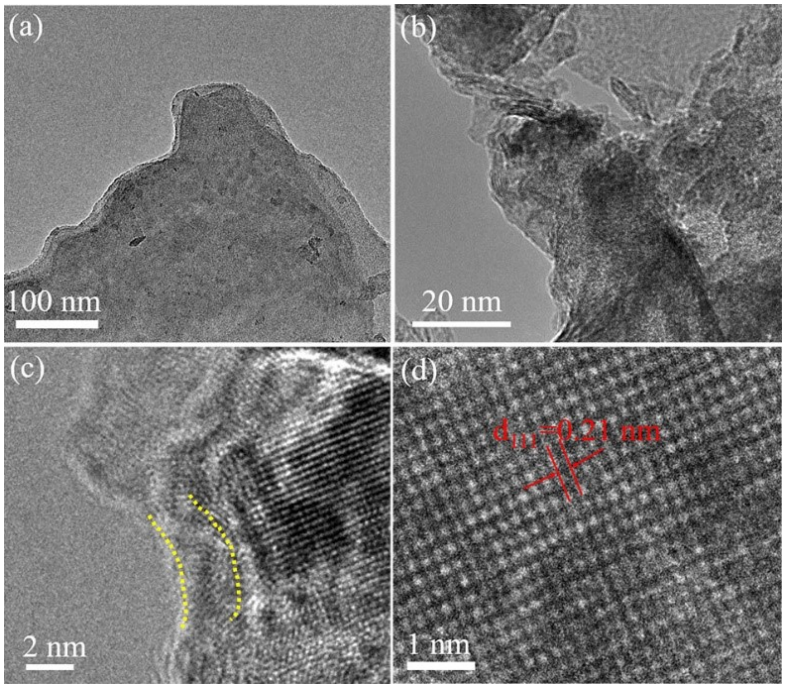

Figure S28. TEM images of Mo-Co_4N catalyst after MOR durability test.

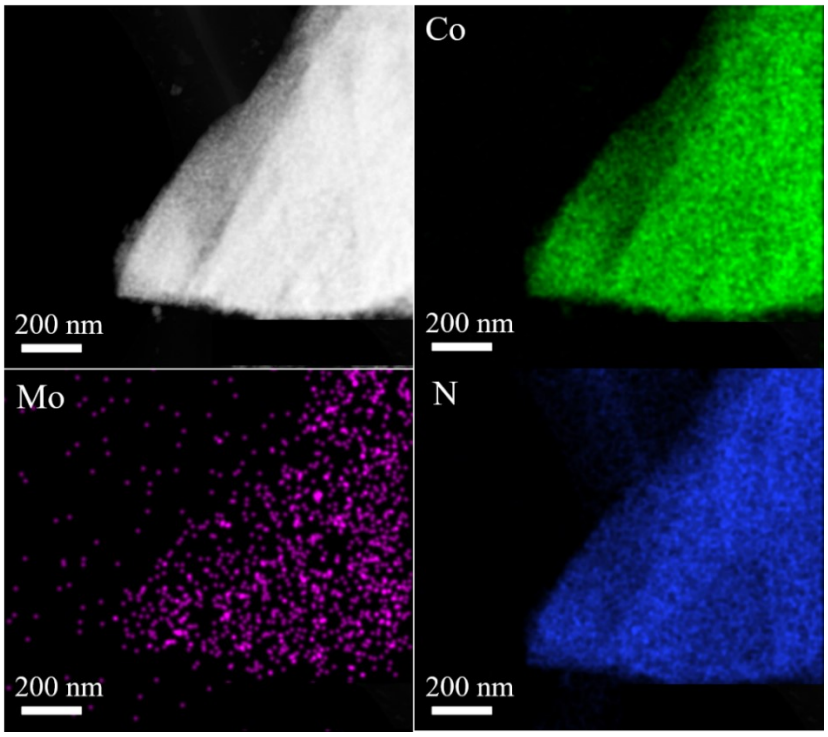

Figure S29. Element mapping images of Mo-Co_4N catalyst after MOR durability test.

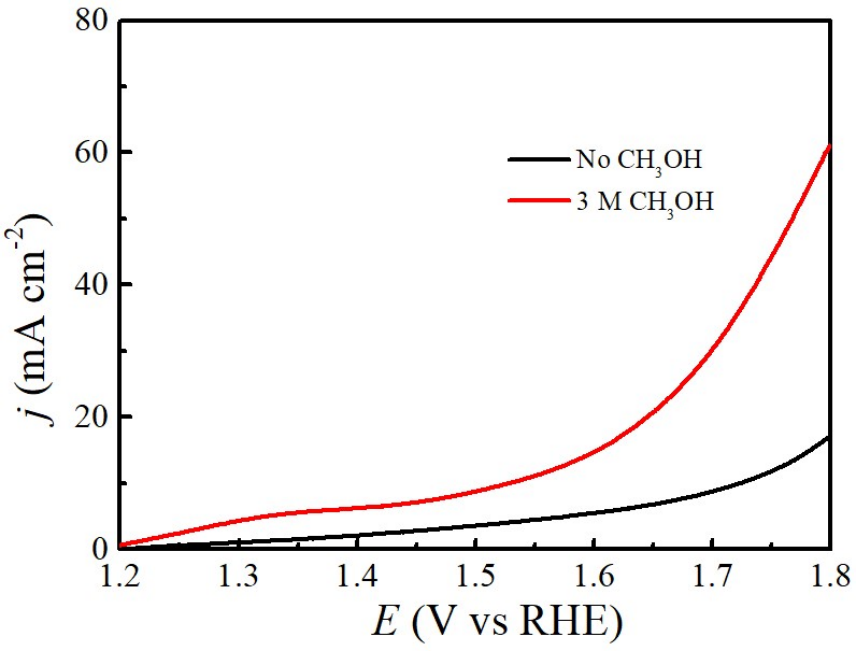

Figure S30. LSV curves of Co_4N couple in 1.0 M KOH with and without CH_3OH in two-electrode system.

Table S1. The metal elements molar ratio of Mo-Co_4N with different dopant ratios detected from ICP measurement.

Element	Co	Mo
Mo_{low}-Co_4N	22.1	1
Mo-Co_4N	18.7	1
Mo_{high}-Co_4N	12.0	1

Table S2. HER performance comparison of this work with report TMNs or Co-based catalysts.

Catalysts	Overpotentials at 10 mA cm^{-2}	Tafel slope (mV dec^{-1})	Reference
Mo-Co_4N	**45**	**42**	**This work**
Mo_2N–Mo_2C/HGr	154	68	*Adv. Mater.* **2018**, 30, 1704156
NiCoN/CC	68	69	*J. Mater. Chem. A* **2018**, 6, 4466-4476
$NiCo_2N$/NF	180	79	*ChemSusChem* **2017**, 10, 4170-4177
MoN@NC	62	54	*ACS Catal.* **2017**, 7, 3540-3547
CoNx/C	133	57	*Nat. Commun.* **2015**, 6,7992
V-Co_4N	37	41	*Angew. Chem. Int. Ed.* **2018**, 57, 5076
$FeNi_3N$	75	98	*Chem. Mater.* **2016**, 28, 6934
Ni_3FeN	158	42	*Adv. Energy Mater.* **2016**, 6, 1502585
Mo-CoP	40	65	*Nano Energy* **2018**, 48, 73-80
Co_9S_8@MoS_2/CNFs	190	110	*Adv. Mater.* **2015**, 27, 4752-4759
Co/CNT	320	79	*Adv. Mater.* **2019**, 31, 1808043
$Co(OH)_2$@HOS/CP	155	71	*Adv. Funct. Mater.* **2020**, 30, 1909610

Table S3. The R_{ct} and R_s of different samples at potential of -0.15 V for HER. R_s related to the series resistance and R_{ct} denotes the charge transfer resistance.

Catalyst	R_s (Ω)	R_{ct} (Ω)
Carbon cloth	2.82	159.5
Co_4N	2.39	40.5
Mo-Co_4N	1.94	2.1

Table S4. The R_{ct} and R_s of different samples at potential of 1.5 V for MOR.

Catalyst	R_s (Ω)	R_{ct} (Ω)
Carbon cloth	3.04	201.7
Co_4N	2.63	3.2
Mo-Co_4N	2.46	2.8

Table S5. Performance comparison of reported two-electrode electrolyzer coupling anodic small organic molecules oxidation reactions and hydrogen production.

Electrode Assembly	Anodic Oxidation Reaction	Potentials at 10 mA cm^{-2}	Reference
Mo-Co_4N||Mo-Co_4N	**Methanol**	**1.427** V	**This work**
$Co(OH)_2$@HOS/CP|| $Co(OH)_2$@HOS/CP	Methanol	1.497 V	*Adv. Funct. Mater.* **2020**, 30, 1909610
$Ni_{0.33}Co_{0.67}(OH)_2$/NF|| $Ni_{0.33}Co_{0.67}(OH)_2$/NF	Methanol	1.65 V@50 mA cm^{-2}	*ChemSusChem* **2020**, 13, 914-921
$Ni(OH)_2$/NF|| $Ni(OH)_2$/NF	Methanol	1.52 V	*Appl. Catal. B* **2021**, 281, 119510
Co_xP@NiCo-LDH/NF|| Co_xP@NiCo-LDH/NF	Methanol	1.43 V	*J Energy Chem.* **2020**, 50, 314-323
Ni-Mo nanotube|| Ni-Mo nanotube	Urea	1.43 V	*Nano Energy* **2019**, 60, 894-902
$Ni(OH)_2$-$NiMoO_x$/NF|| $Ni(OH)_2$-$NiMoO_x$/NF	Urea	1.42 V	*Adv. Energy Mater.* **2019**, 9, 1902703
Ni_2P/Ni||Pt/C	Urea	1.47 V	*Nano Research* **2021**, 14, 1405-1412
MoO_2-FeP@C||MoO_2-FeP	5-hydroxymethyl furfural	1.486 V	*Adv. Mater.* **2020**, 32, 2000455
hp-Ni/NF||hp-Ni/NF	5-hydroxymethyl furfural	1.50 V	*ACS Catal.* **2017**, 7, 4564
NiSe@NiO_x|| NiSe@NiO_x	5-hydroxymethyl furfural	1.50 V	*Appl. Catal. B* **2020**, 261, 118235
Ni_3N@C/NF|| Ni_3N@C/NF	5-hydroxymethyl furfural	1.46 V	*Angew. Chem. Int. Ed.* **2019**, 131, 16042
CoNW/NF||CoNW/NF	5-hydroxymethyl furfural	1.504 V	*Green Chem.* **2019**, *21*, 6699